

An investigation of eddy-current damping of multi-stage pendulum suspensions for use in interferometric gravitational wave detectors

M. V. Plissi

Institute for Gravitational Research, University of Glasgow, Glasgow G12 8QQ, Scotland, United Kingdom

C. I. Torrie and M. Barton

California Institute of Technology, Pasadena, California 91125

N. A. Robertson

Edward L. Ginzton Laboratory, Stanford University, Stanford, California and Institute for Gravitational Research, University of Glasgow, Glasgow G12 8QQ, Scotland, United Kingdom

A. Grant, C. A. Cantley, and K. A. Strain

Institute for Gravitational Research, University of Glasgow, Glasgow G12 8QQ, Scotland, United Kingdom

P. A. Willems and J. H. Romie

California Institute of Technology, Pasadena, California 91125

K. D. Skeldon

Optics Group, Department of Physics and Astronomy, University of Glasgow, Glasgow G12 8QQ, Scotland, United Kingdom

M. M. Perreur-Lloyd, R. A. Jones, and J. Hough

Institute for Gravitational Research, University of Glasgow, Glasgow G12 8QQ, Scotland, United Kingdom

(Received 27 May 2004; accepted 25 July 2004; published 29 October 2004)

In this article we discuss theoretical and experimental investigations of the use of eddy-current damping for multi-stage pendulum suspensions such as those intended for use in Advanced LIGO, the proposed upgrade to LIGO (the US laser interferometric gravitational-wave observatory). The design of these suspensions is based on the triple pendulum suspension design developed for GEO 600, the German/UK interferometric gravitational wave detector, currently being commissioned. In that detector all the low frequency resonant modes of the triple pendulums are damped by control systems using collocated sensing and feedback at the highest mass of each pendulum, so that significant attenuation of noise associated with this so-called local control is achieved at the test masses. To achieve the more stringent noise levels planned for Advanced LIGO, the GEO 600 local control design needs some modification. Here we address one particular approach, namely that of using eddy-current damping as a replacement or supplement to active damping for some or all of the modes of the pendulums. We show that eddy-current damping is indeed a practical alternative to the development of very low noise sensors for active damping of triple pendulums, and may also have application to the heavier quadruple pendulums at a reduced level of damping. © 2004 American Institute of Physics. [DOI: 10.1063/1.1795192]

I. INTRODUCTION

The triple pendulum suspension system¹ developed for the main mirrors (test masses) in GEO 600 is designed to minimize the effects of thermal and seismic noise on the suspended test masses. The effect of thermal noise is minimized by using fused silica fibres in the final stage of the suspension. A multiple pendulum system gives good seismic isolation in the horizontal direction. However, because there is unavoidable cross coupling of vertical to horizontal motion of the test mass, vertical isolation is also important. In the GEO 600 test mass suspension system this is achieved by the incorporation of two steel cantilever blade spring stages in the upper two stages of the suspension. In order to achieve good isolation and low thermal noise it is required that the resonant modes of such suspension systems possess high quality (Q) factors, which if uncontrolled would lead to large

coupling of seismic noise to mirror motion at the resonant frequencies of the suspension. Large motions of the mirrors of the interferometer make the acquisition of lock of the optical system difficult and require a large operating range for the feedback actuators used to maintain the interferometer locked to a fringe. Due to dynamic range limits a large operating range raises the noise floor of the actuator drive and is, therefore, undesirable. Thus control systems are required in order to damp the low frequency motion of the mirrors. In GEO 600 we designed the suspension and its active damping or local control system such that all the low frequency modes (frequencies in the range ~ 0.4 Hz to ~ 4 Hz) are damped to a Q of around 5, thus reducing the overall motion at the resonant frequencies, and giving acceptable settling times of the pendulum modes. The local control is applied using six collocated optical sensing and electromagnetic feedback units acting at the highest mass of

each pendulum and the suspension is designed so that all the low frequency modes are well coupled to this mass.

Electronic damping of the pendulum modes is a method that has yielded good results in suspension systems and avoids a noise penalty in the gravitational wave detection band if the sensors and actuators chosen are of sufficiently low noise and are adequately isolated from the test masses. In particular the use of multi-stage pendulums can provide passive filtering of the effects of electronic noise, which combined with electronic filtering can ensure that the noise performance of the detector is not limited by the local control system, as demonstrated in GEO 600. The suspension design for Advanced LIGO² is based on the GEO 600 design, developed to have improved noise performance extending to lower frequencies. As discussed in a previous paper³ the more stringent noise requirements of Advanced LIGO would not be met using sensors of the type currently in use in LIGO and GEO 600, even with the extension to a quadruple pendulum suspension for the most sensitive mirrors. This is assuming fairly simple control systems and a damping level similar to that already in use in these interferometers.

Development of lower noise sensors is one way to approach this problem, and this is currently under investigation. An alternative method for damping the pendulum modes is to use eddy-current damping. This has the advantage of being a totally passive damping technique thus avoiding additional electronic noise. However, for it to be practicable, questions of thermal noise as well as damping performance and isolation have to be considered.

Eddy-current damping has been considered for use in other interferometric gravitational wave detectors. The VIRGO (French-Italian) group have previously investigated the possible adverse effect of increased thermal noise.⁴ A triple pendulum isolation system incorporating eddy-current dampers has been developed in Japan.⁵ In this system the top and middle mass of the triple pendulum are made of copper, and the magnets to apply damping at these two masses are themselves supported on flexible mounts with a resonant frequency above the pendulum mode to be damped but below the gravitational-wave band. The use of such flexible mounts ensures that the eddy-current damping does not compromise the seismic isolation of the triple pendulum at frequencies above the resonant frequencies of the mounts. The isolation for a high quality factor triple pendulum suspension will improve as f^6 above the low frequency resonances. Consider eddy-current damping introduced between the top mass and a mass rigidly attached to the point of suspension. Due to the viscous nature of the damping this will compromise the isolation by one factor of f to f^5 . By the use of a flexible mount, this factor of f is regained at frequencies above the resonant frequency of the mount, and this is one of the significant design features in the Japanese system. It has not been necessary to apply such a technique in our design since the isolation requirements are adequately met, even allowing for the change in dependence on frequency at higher frequencies. A consequence of the Japanese design is that thermal noise will be introduced at both the top and more particularly the middle mass. In our system we propose that eddy-current damping is applied only at the topmost mass of a triple or

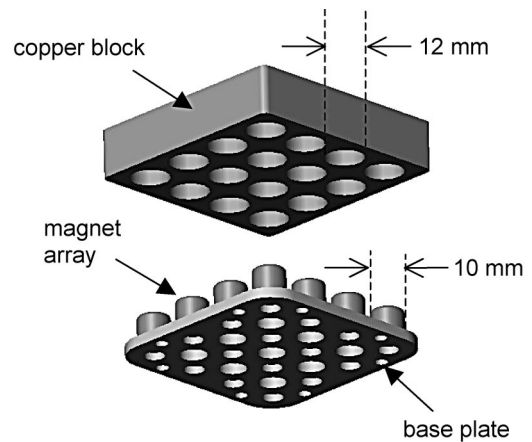


FIG. 1. A schematic of the magnet array and the bulk copper block used for the initial set of measurements.

quadruple pendulum, thus minimizing the residual motion at the bottom mass due to thermal noise. The effectiveness of such damping applied only at the top mass relies on all the low frequency modes of the pendulum being well coupled as mentioned above. In this paper we present experimental results of eddy-current damping applied to a triple pendulum in longitudinal and vertical directions, comparing these results with predictions from a MATLAB⁶ model of the suspension.¹ We also present results from an investigation of an improved eddy-current damper design tested on a single pendulum. Based on these results we discuss the feasibility of applying eddy-current damping in Advanced LIGO for both triple and quadruple pendulums, taking into account issues of isolation, thermal noise, and the level of damping.

II. INITIAL DESIGN OF EDDY-CURRENT DAMPER

Our design of eddy-current damper is based on the idea of an array of magnets moving inside an array of holes cut in a copper block (see Fig. 1). The magnets were arranged with opposing polarities on the metal base plate in order to reduce the overall dipole field and hence reduce potential coupling to any external magnetic fields. In addition, arranging them in this way enhances the overall damping produced (see Sec. V). These magnets were cylinders of 10 mm diameter and 10 mm thick and made from sintered Neodymium-Iron-Boron (NdFeB). Sintered NdFeB has the highest remanence of any commercially available magnetic material, the magnet chosen for the experiment (grade N35H) having an assumed remanence of 1.21 T.⁷ The penetration distance of the magnets into the copper block (>99.9% Cu) was 8.5 ± 0.5 mm, this being the maximum practical penetration distance for this particular arrangement. The magnet array has its motion retarded such that the retardation force is proportional to the velocity of the array, a form of viscous damping. Standard electromagnetic theory can be used to estimate the eddy-current damping force and this can be compared with experimental investigations. The theoretical background to eddy-current damping is outlined in the Appendix where we consider the effect of a single magnet moving within a copper block.

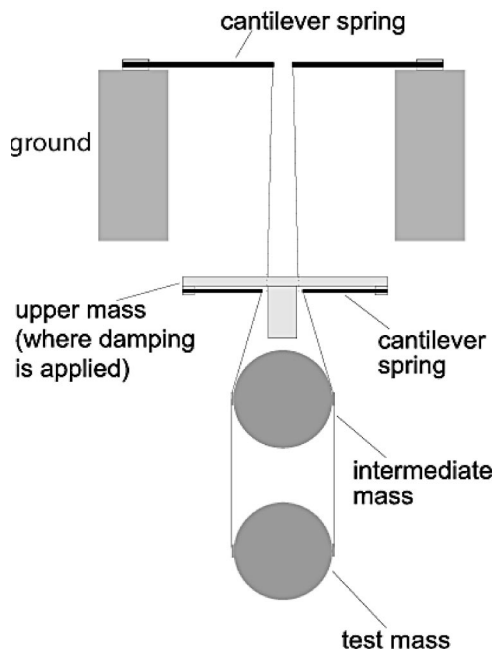


FIG. 2. A schematic of the triple pendulum suspension. The damping is applied between the ground and the upper mass.

III. EXPERIMENTAL RESULTS

A triple pendulum suspension that is similar in design to a GEO 600 test mass suspension was used (see Fig. 2). The mass of each stage of the pendulum is ~ 6 kg and there are two cantilever spring stages for enhanced vertical isolation. A full description of the suspension can be found in an earlier paper.¹ Note that the longitudinal direction is the axis along which motions due to gravitational waves are sensed, and is, therefore, the most important direction for isolation. Significant vertical isolation is also important because of the relatively poorer seismic isolation of the pendulum in this direction and the cross coupling of vertical motion to longitudinal, which will be inevitable with a long baseline interferometer due to the curvature of the Earth. Two 4×4 magnet arrays, of the type illustrated in Fig. 1, were mounted on the uppermost mass for investigating vertical and longitudinal damping. The copper block was mounted on a support structure rigidly attached to the point of suspension of the triple pendulum. The layout with one of the damping units in place is shown in Fig. 3. It should be noted that in the final system it would be advisable to mount the magnet arrays on the support structure. This arrangement would minimize the effect of any coupling to any ambient fields that could in effect cause a spurious noise input, albeit at a low level and two (or more) stages removed from the test mass. Three x - y - z piezoelectric actuators that were mounted on the support frame drove the suspension in a swept sine mode and the transfer function was measured between “ground” and the uppermost mass of the suspension. B & K accelerometers (Uni Gain Type 4379) were used with their outputs being amplified and passed to a network analyzer. Care was taken in aligning the copper block so that there was no metal-to-metal contact. This was checked with a continuity sensor. The copper block was electrically isolated from the ground and the magnet array was electrically connected to ground

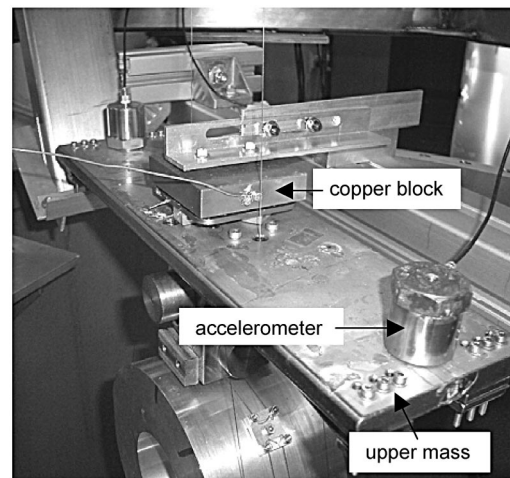


FIG. 3. Photograph of the revised experimental set-up for the vertical damping measurements. The magnet array is mounted on the upper mass of the suspension. The copper block, arrowed, is positioned over the array. An accelerometer is shown positioned at either end of the mass.

via the support structure. Contact between the magnet array and copper block completed a circuit and triggered a buzzer. All of the following measurements were performed in air.

A. Vertical damping

Vertical transfer functions were measured before and after positioning the copper block inside the magnet array. In the initial setup the damping array was positioned, for convenience, close to the end of the upper mass. It was realized that with the damper in this position there was preferential damping of roll motion. The damper was then repositioned close to the center of the upper mass and the measurements repeated and it was discovered that the vertical damping was a factor of ~ 4 more effective than it was previously. Subsequent theoretical analysis has confirmed the degradation in vertical damping expected when a damper is shifted away from the axis of the center of mass. In order to discriminate against the sensing of roll motion, two accelerometers (matched to within $\sim 3\%$) were placed at opposite ends of the upper mass and connected so that the output of one was subtracted from that of the other. With this arrangement the sensing of roll motion was minimized and vertical motion was preferentially sensed. This is indicated in Fig. 4 where the transfer function over the two lowest vertical modes is shown.

We see that the modes are well damped and from the experimental data we estimate a value of $Q=5.3 \pm 0.5$ for the lowest mode and $Q=6.4 \pm 0.5$ for the higher mode. For comparison the undamped Q 's were estimated to be ~ 55 and ~ 90 , respectively, for these two modes. Using a MATLAB model of a GEO 600 suspension,¹ modified to approximate to our current experimental arrangement, we can calculate the damping constant b for which a force applied between the “ground” and the upper mass of b multiplied by their relative velocities gives values of Q close to those listed above. The resulting transfer function is also shown in Fig. 4 for a b of 28 kg/s. Apart from a small difference in the magnitude of the transfer function the agreement with ex-

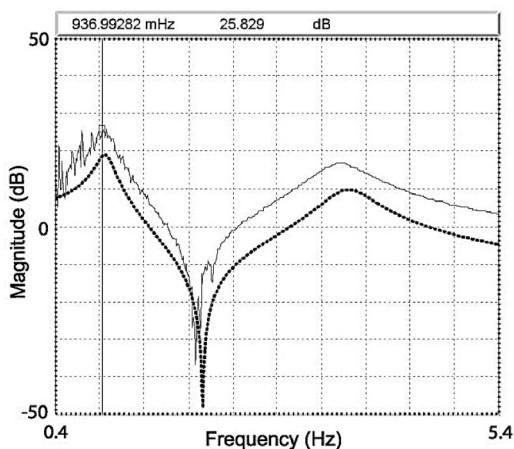


FIG. 4. Comparison between the experimental vertical transfer function (solid) and a MATLAB model (dashed) between the ground and the upper mass. In the MATLAB plot a damping constant of 28 kg/s has been assumed.

perimental data is good. The highest vertical frequency mode of this triple pendulum suspension, not shown, is at ~ 25 Hz. This mode is associated primarily with the motion of the lowest mass moving with respect to the mass above it and is much higher than the other modes since the lowest stage of the pendulum has no soft vertical springs. This mode is relatively uncoupled from the two lower frequency modes and therefore remains undamped.

B. Longitudinal damping

Longitudinal transfer function measurements (with the piezoelectric actuators driving in the longitudinal direction) were taken with the array mounted at the center of the side of the uppermost mass. The top array was removed for these measurements and the accelerometers were aligned to be most sensitive in the longitudinal direction. Figure 5 shows the longitudinal transfer function, measured with a single 4×4 array, over a frequency range covering the three longitudinal modes of the suspension. The estimated Q of the three modes (with increasing mode frequency) is 6.0, 5.2,

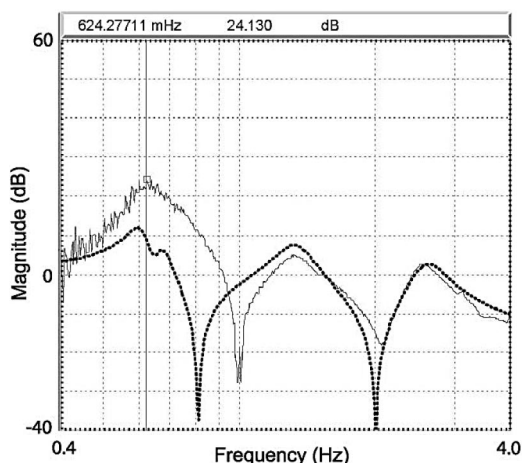


FIG. 5. Comparison between the experimental longitudinal transfer function (solid) and MATLAB model (dashed) between the ground and the upper mass. In the MATLAB plot a damping constant of 26 kg/s has been assumed.

and 6.5 (± 0.5) (For comparison the undamped Q 's were estimated to be ~ 30 , ~ 50 , and ~ 85 , respectively, for these three modes.) A MATLAB model of the suspension is also shown in Fig. 5 for a damping constant of 26 kg/s for which we obtain Q 's of these modes, of 9.4, 5.4, and 7.7. There is, in general, reasonable agreement between the experimental and theoretical results. The lowest and highest longitudinal modes are each contaminated by a pitch mode (clearly apparent for the lowest mode in the MATLAB plot). Each of these peaks is therefore composed of two damped resonances coupled together. As a consequence the effective Q 's, for these longitudinal modes, estimated from the experimental transfer function are lower than the MATLAB prediction. The mismatch in the position of the first zero in the transfer function is most likely a result of the experimental setup having a different level of pitch-longitudinal coupling compared to that predicted by the model.

IV. APPLICATION OF EDDY-CURRENT DAMPING TO THE SUSPENSIONS IN ADVANCED LIGO

We have demonstrated experimentally that eddy-current damping applied to the uppermost mass of a triple pendulum can be used to damp all the low frequency modes in longitudinal and vertical directions, as predicted by our model. Thus we expect that application of further arrays suitably positioned around the uppermost mass could be used to damp all the other low frequency modes of such a suspension. We can extend this argument to the quadruple suspension design to be used for the most sensitive optics in Advanced LIGO. Our modeling, and our experience with active damping of a prototype quadruple suspension, where the damping was applied at the uppermost mass, leads us to conclude that in principle eddy-current damping could also be applied in a quadruple pendulum design. However, we need to consider the requirements on the level of damping needed and on the residual thermal noise that can be tolerated for each suspension.

The motion due to thermal noise associated with eddy-current damping can be calculated as follows. For a damping force of magnitude b times velocity, the power spectral density of the thermal driving force is given by $F^2 = 4k_b T b$, where k_b is Boltzmann's constant, and T is temperature.⁸ Thus F (in units of $N/\sqrt{\text{Hz}}$) can be calculated for a given value of b . To estimate the resulting displacement of the mirror due to this force, we use the MATLAB model to solve for the transfer function of force applied at the top mass to displacement of the mirror in the appropriate direction.

In Advanced LIGO there are several different types of optics that require low noise suspensions. For the most sensitive optics (the test masses) a quadruple suspension is required, where the design has been chosen to aim to reach a target noise contribution at the test mass from residual seismic noise of not greater than $1 \times 10^{-19} \text{ m}/\sqrt{\text{Hz}}$ at 10 Hz. For certain other optics such as the mirrors for the modecleaner used to reduce laser beam geometry fluctuations, and for the mirrors used for optical recycling in the interferometer, the noise requirements are relaxed by a factor of order 100. For these mirrors a triple pendulum suspension can meet the re-

quirements. Since the optics are of different mass, the overall suspension mass varies between designs, and this is a significant factor for consideration of damping. It should be noted that the overall mechanical isolation required to reduce the seismic noise contribution to the required levels is achieved by suspending the quadruple or triple suspension from a two-stage active isolation platform.⁹

The lightest of the sensitive optics are the modecleaner mirrors, which are suspended as triple pendulums, each stage having a mass of 3 kg, and thus the total mass of the suspension is 9 kg. This is approximately half that of the triple suspension used in our experimental investigations. The damping requirements for Advanced LIGO as currently stated are to give settling times of 10 s or less for all the low frequency modes. To achieve such settling times in the longitudinal direction, for example, we predict that a damping constant of ~ 4.5 kg/s is adequate, and such a value could be achieved by a much smaller magnet array than already investigated experimentally. The residual longitudinal thermal noise due to such damping would lie a factor of ~ 3.5 below the overall noise requirement for the longitudinal motion of this optic that is set at 3×10^{-17} m/ $\sqrt{\text{Hz}}$ at 10 Hz. Similar values of damping applied in the other directions should also satisfy the requirements.

The recycling mirrors, which are also suspended as triple pendulums, each stage having a mass of 12 kg, with a total suspension mass of around 36 kg, and thus the total mass is around four times that of the modecleaner suspensions. In addition, there are differences in the lengths of each stage and in the amount of coupling between modes. From our model, we find that to damp the longitudinal modes of the recycling mirror to give a 10 s settling time requires a damping constant of ~ 40 kg/s. To achieve such a level of damping, two arrays each somewhat smaller than that already investigated could be used. If suitably positioned, adequate damping of the yaw modes could also be achieved at the same time. We have checked that the thermal noise due to such damping lies below the noise requirements for this optic. Other similar arrays suitably placed around the upper mass could be used to adequately damp the other degrees of freedom.

The baseline design for the test mass suspension is to have a test mass of 40 kg, and an overall suspension mass of around 124 kg. Thus considerably higher damping constants are required to achieve 10 s settling times. For example, for our current design a damping constant of around 190 kg/s would be needed in the longitudinal direction to achieve a 10 s damping time. Providing this level of damping would be a very challenging practical problem. However, for the vertical direction a more modest value of ~ 80 kg/s would give a settling time of ~ 10 s. Thus, for example, using two 4×4 arrays similar to those already investigated, with a total b of 56 kg/s, would give a settling time of ~ 14 s. The thermal noise resulting from this latter amount of damping is estimated to give a residual motion coupled into the longitudinal direction of $\sim 4.5 \times 10^{-20}$ m/ $\sqrt{\text{Hz}}$ at 10 Hz.

Finally, the isolation requirements should be adequately met, for both triple and quadruple suspensions despite the reduction in the isolation of the first stage of the pendulum

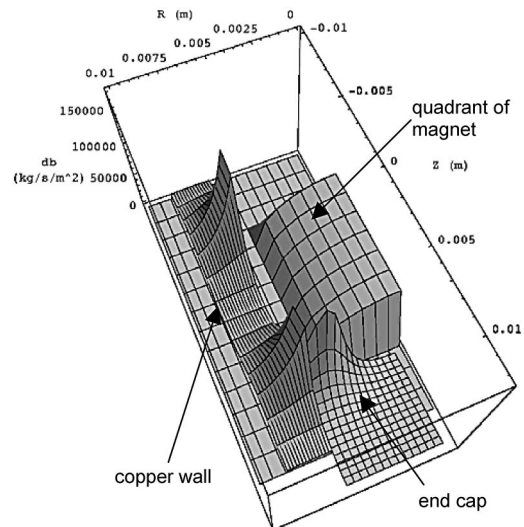


FIG. 6. The contribution to the damping coefficient from an annulus of radius R and longitudinal position Z relative to the magnet. Integrating with respect to R and Z over all regions where there is copper gives the total damping in kg/s/m^2 . A three-dimensional (3D) representation of one quadrant of the magnet has been superimposed as a visual guide, but note that the vertical axis of the main plot is not length. The clearance around the magnet is 1 mm and the end cap is 1 mm from the end of the magnet. It is apparent that most of the damping is generated in a small volume near the shoulders of the magnet so that copper in other places will be less effective.

due to the eddy-current damper. For example, in the vertical direction, for the quadruple suspension, the introduction of eddy-current damping of magnitude $b=56$ kg/s increases the transmissibility at 10 Hz by a factor of around 1.4 from that given by an undamped system, to a value of $\sim 2.7 \times 10^{-4}$. When this is combined with the expected vertical noise input at the top of the suspension, and an assumed cross-coupling factor of 1×10^{-3} , and added in quadrature to the residual motion due to the vertical damping thermal noise, the resulting contribution to noise at the optics is estimated to be 7×10^{-20} m/ $\sqrt{\text{Hz}}$.

Thus eddy-current damping could be used to adequately damp the triple pendulum suspensions that are proposed for Advanced LIGO, and could approach the required level of damping for some of the degrees of freedom of the much heavier quadruple pendulums.

V. FURTHER DEVELOPMENTS

For practical reasons in the overall design of the suspension and isolation system in Advanced LIGO it is advantageous to keep the mass of the damping units as low as possible. Therefore, an improved geometry for the copper block was analyzed. The full analysis, carried out for one magnet moving within a copper block is given in the Appendix. In order to see which regions of copper contribute significantly to the damping we can plot the result of integrating over r , θ , and z (i.e., the volume of the magnet), Fig. 6. The complex surface at the front and left gives the contribution to the eddy-current damping of axial motion from an annulus of radius R and axial position Z within the copper block. The clearance around the magnet is 1 mm and the piece on the left represents the copper wall. The piece at the front represents the end cap, again with a clearance of 1 mm. It is

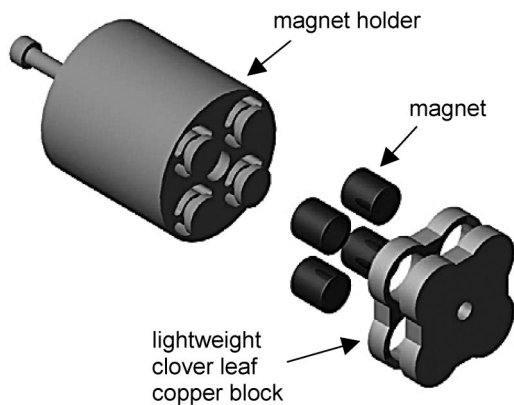


FIG. 7. Exploded view of a 2×2 array showing the lightweight clover leaf design for the copper block (LIGO-D030243).

immediately clear that only the copper off the shoulders of the magnet contributes significantly. Copper around the waist of the magnet and along the axis contributes little to the damping. A lightweight “clover leaf” design, for a 2×2 array (see Fig. 7) was developed based on this analysis. An array such as this could be used to passively damp one or more degrees of freedom of a light triple pendulum suspension. The design could be extended to larger arrays for heavier pendulums.

This array was used on a single pendulum suspension of mass 6 kg and a damping constant of 5.5 kg/s was estimated from a ringdown measurement. The pendulum was excited and the time it took for the amplitude to decay to $1/e$ of the peak amplitude was measured. The Q was estimated directly from this and used to calculate the damping constant. The calculation is simpler in this case because of the single stage used in the suspension (for a multi-stage pendulum an effective mass must be used). The experiment was repeated using a bulk copper design (a design in which no effort was made to economize on the amount of copper used) whereby a damping constant of 5.8 kg/s was obtained. Based on the numerical model outlined in the Appendix the damping, for this design, was expected to range from 3.9 kg/s (for a minimum wall thickness the whole way round) to 5.9 kg/s (assuming a large wall thickness). From the analysis it is readily apparent that there is little point in making the walls thicker than 2 to 3 mm. The experimental result, therefore, compares favorably with the model. It should also be noted that for these measurements the magnets were placed on stalks so that they fully penetrated the copper block thus ensuring that both ends of the magnets contributed to the overall damping. An interim design, termed medium weight copper, was also tested. This design was essentially a clover leaf design but with the middle section retained. The main results are summarized in Table I. The bulk copper design is actually slightly inferior to this interim design because the depth of the hole is 1 mm or so less than optimum and some potential damping near the outer end of the magnet is wasted, even with stalks. Comparing these results with those taken with a 4×4 array confirms that the eddy-current damping scales linearly with the size of the array, as expected.

In summary we have confirmed that the scaling between the different sizes of array applies as expected, that the light-

TABLE I. Experimentally determined damping constants for the different configurations of 2×2 arrays tested (clover leaf, medium weight and bulk copper). The second entry refers to a measurement taken with the magnetic poles aligned in the same direction. For the other cases the magnets were arranged with opposing polarities. Included for comparison is an extrapolation, to a 2×2 array, from a measurement with a single magnet. All the b values entered above correspond to an upper bound of a set of measurements obtained for each damping configuration.

eddy-current damping configuration	b (kg/s)
‘Clover leaf’, 2×2 array	5.5
‘Clover leaf’ (with magnets aligned in same direction), 2×2 array	3.3
Bulk copper, 2×2 array	5.8
Medium weight copper, 2×2 array	6.7
‘Clover leaf’ (extrapolation from a single magnet), 2×2 array	4.8

weight clover leaf design shows a damping performance close to that of bulk copper and that the experimental measurements fit well with predictions.

In seeking ways in which we could further improve the damping performance for the quadruple suspensions other materials or schemes were considered. The effectiveness of eddy-current damping depends on the resistance of the current paths in the conductive material. The lower the resistance (or the higher the conductivity) the greater the damping. In order to improve the damping, therefore, one should select the highest conductivity material. At room temperature only silver is a better conductor than copper and then only by $\sim 5\%$.¹⁰ Therefore, assuming a linear relationship between conductivity and damping performance the improvement in selecting silver over copper is marginal. Beryllium is a better conductor than either of these materials but only below 180 K. At these low temperatures one can also consider superconductors. The highest temperature superconductor currently known is a mercury-based cuprate with a transition temperature of around 130 K at atmospheric pressure.¹¹ Peltier devices would not provide sufficient cooling and although miniature electromechanical refrigeration units (cryocoolers) exist for these low temperatures they are inherently noisy. Pulse tube cryocoolers¹² have typically two orders of magnitude lower vibration amplitudes than standard types; however, their vibration levels are still higher than the noise requirement for Advanced LIGO.

ACKNOWLEDGMENTS

The authors would like to thank Bill Edelstein, David Shoemaker, and Jim Faller for their helpful advice and interest in this work. The authors acknowledge the financial support of the University of Glasgow and the PPARC. N. A. Robertson was supported by the National Science Foundation under NSF Grant PHY-0140297. C. I. Torrie, M. Barton, P. A. Willems, and J. H. Romie were supported by the National Science Foundation under NSF Grant No. PHY-0107417.

APPENDIX: CALCULATION OF DAMPING FORCES

Consider the effect of a single magnet moving within a copper block. In general, an infinitesimal element of magnetic dipole moment $d\mathbf{m}$ at source coordinates (x, y, z) produces a contribution to magnetic field \mathbf{B} at field coordinates (X, Y, Z) nearby given by

$$d\mathbf{B} = -\frac{\mu_0}{4\pi} \nabla \left(d\mathbf{m} \cdot \nabla \frac{1}{r_{sf}} \right), \quad (\text{A1})$$

where r_{sf} is the vector from the source point to the field point. If the source moves at velocity v , then the contribution to EMF along a line element $d\mathbf{l}$ at (X, Y, Z) is

$$d\xi = d\mathbf{B} \times \mathbf{v} \cdot d\mathbf{l}. \quad (\text{A2})$$

We wish to apply this to the interaction between a cylindrical magnet oriented, magnetized and moving along the z axis and the walls, assumed spherically symmetric, of a surrounding cavity. If the magnetic moment per unit volume of the magnet material is M , each infinitesimal volume element dV of material contributes $d\mathbf{m} = dV(0, 0, M)$, and Eq. (A1) becomes

$$d\mathbf{B} = \frac{\mu_0 M dV}{4\pi} \begin{bmatrix} \frac{3(X-x)(Z-z)}{((X-x)^2 + (Y-y)^2 + (Z-z)^2)^{5/2}} \\ \frac{3(Y-y)(Z-z)}{((X-x)^2 + (Y-y)^2 + (Z-z)^2)^{5/2}} \\ \frac{2(Z-z)^2 - (X-x)^2 - (Y-y)^2}{((X-x)^2 + (Y-y)^2 + (Z-z)^2)^{5/2}} \end{bmatrix}. \quad (\text{A3})$$

For convenience we will use cylindrical coordinates defined by

$$(x, y, z) = (r \cos \theta, r \sin \theta, z) \quad (\text{A4})$$

and

$$(X, Y, Z) = (R \cos \Theta, R \sin \Theta, Z). \quad (\text{A5})$$

Now consider a line element that is part of a circle of radius R in the xy plane, centered on the z axis

$$d\mathbf{l} = d\Theta(-R \sin \Theta, R \cos \Theta, 0), \quad (\text{A6})$$

and a velocity $\mathbf{v} = (0, 0, v)$. Then Eq. (A2) becomes

$$d\xi = \frac{3\mu_0 v M dV R d\Theta (z-Z)(R-r \cos(\Theta-\theta))}{4\pi (r^2 + R^2 + z^2 - 2zZ + Z^2 - 2rR \cos(\Theta-\theta))^{5/2}}. \quad (\text{A7})$$

To calculate the EMF around the full circle of radius R , Eq. (A7) must be integrated over Θ from 0 to 2π . Fortunately, as might be expected from symmetry, $d\xi$ depends only on the

difference of angles. Therefore, it is convenient to eliminate θ by making the substitution $\phi = \Theta - \theta$ and integrating from 0 to 2π . Note that the solution involves elliptic integral functions.

Now, because of the axial symmetry, the eddy-currents flow in the same direction as the EMF. Therefore, if we consider a toroid of length $2\pi R$ and infinitesimal cross-sectional area $dRdZ$ following the circular path along ξ the current flow in this toroid can be calculated independently of any other. The contribution to electrical power dissipation is

$$dP = \frac{dRdZ\xi(R, Z)^2}{2\pi R\rho}, \quad (\text{A8})$$

where ρ is the resistivity of the walls of the cavity.

The contribution to the eddy-current damping constant is

$$db = \frac{dP}{v^2} = \frac{dRdZ\xi(R, Z)^2}{2\pi R\rho v^2}. \quad (\text{A9})$$

Finally, to calculate the total eddy-current damping b , we put

$$dV = drrd\theta dz, \quad (\text{A10})$$

where V is the volume and integrate over r , θ , z , R , and Z . This needs to be done numerically.

¹M. V. Plissi, C. I. Torrie, M. E. Husman, N. A. Robertson, K. A. Strain, H. Ward, H. Lück, and J. Hough, *Rev. Sci. Instrum.* **71**, 2539 (2000).

²P. Fritschel, *Proc. SPIE Vol. 4856, Gravitational Wave Detection*, edited by M. Cruise and P. Saulson (SPIE, Bellingham, WA, 2003), p. 282.

³N. A. Robertson, G. Cagnoli, D. R. M. Crooks, E. Elliffe, J. E. Faller, P. Fritschel, S. Gossler, A. Grant, A. Heptonstall, J. Hough, H. Lück, R. Mittleman, M. Perreux-Lloyd, M. V. Plissi, S. Rowan, D. H. Shoemaker, P. H. Sneddon, K. A. Strain, C. I. Torrie, H. Ward, and P. Willems, *Class. Quantum Grav.* **19**, 4043 (2002).

⁴G. Cagnoli, L. Gammaitoni, J. Kovalik, F. Marchesoni, and M. Punturo, *Rev. Sci. Instrum.* **69**, 2777 (1998).

⁵K. Tsubono, A. Araya, K. Kawabe, S. Moriwaki, and N. Mio, *Rev. Sci. Instrum.* **64**, 2237 (1993).

⁶MATLAB for Windows, copyright 1984-2002, The Mathworks Inc. Version 6.5 (2002).

⁷<http://www.magdev.co.uk/material.htm>.

⁸P. R. Saulson, *Phys. Rev. D* **42**, 2437 (1990).

⁹R. Abbott, R. Adhikari, G. Allen, D. Baglino, C. Campbell, D. Coyne, E. Daw, D. DeBra, J. Faludi, P. Fritschel, A. Ganguli, J. Giaime, M. Hammond, C. Hardham, G. Harry, W. Hua, L. Jones, J. Kern, B. Lantz, K. Lilienkamp, K. Mailand, K. Mason, R. Mittleman, S. Nayfeh, D. Ottaway, J. Phinney, W. Rankin, N. Robertson, R. Scheffler, D. H. Shoemaker, S. Wen, M. Zucker, and L. Zuo, *Class. Quantum Grav.* **21**, S915 (2004).

¹⁰*Handbook of Chemistry and Physics*, edited by D. R. Lide (CRC Press Inc., Boca Raton, FL, 1993).

¹¹S. H. Yun and J. Z. Wu, *Appl. Phys. Lett.* **68**, 862 (1996).

¹²T. Tomaru, T. Suzuki, T. Haruyama, T. Shintomi, A. Yamamoto, Y. Ikushima, T. Koyama, and R. Li, *28th International Cosmic Ray Conference*, edited by T. Kajita, Y. Asaoka, A. Kawachi, Y. Matsubara, and M. Sasaki (Universal Academy Press Inc., Tokyo, 2003), p. 3127.